

# Microwave-Assisted Preparation of White Fluorescent Graphene Quantum Dots as a Novel Phosphor for Enhanced White-Light-Emitting Diodes

Zhimin Luo, Guangqin Qi, Keyu Chen, Min Zou, Lihui Yuwen, Xinwen Zhang,\*  
Wei Huang,\* and Lianhui Wang\*

Graphene quantum dots (GQDs) with white fluorescence are synthesized by a microwave-assisted hydrothermal method using graphite as the precursor. A solution-processed white-light-emitting diode (WLED) is fabricated using the as-prepared white fluorescent GQDs (white-light-emitting graphene quantum dots, WGQDs) doped 4,4-bis(carbazol-9-yl)biphenyl as the emissive layer. White-light emission is obtained from the WLED with 10 wt% doping concentration of WGQDs, which shows a luminance of 200 cd m<sup>-2</sup> at the applied voltage of 11–14 V. Importantly, an external quantum efficiency of 0.2% is achieved, which is the highest among all the reported WLED based on GQDs or carbon dots. The results demonstrate that WGQDs as a novel phosphor may open up a new avenue to develop the environmentally friendly WLEDs for practical application in solid-state lighting.

## 1. Introduction

White-light-emitting diodes (WLEDs) are considered the most promising light source in the future due to their advantages such as low power consumption, high luminous efficiency, and long lifetime.<sup>[1–3]</sup> WLEDs based on whole organic materials are relatively low-cost and easy for large-scale production, but their environmental stability is low and device lifespan is limited.<sup>[4–6]</sup> Semiconductor nanocrystals, especially semiconductor quantum dots, have attracted increasing attention in

the application of WLEDs due to their high fluorescent quantum yield, narrow emission bandwidth, and resistance to the photobleaching.<sup>[3,7–9]</sup> Integration of quantum dots into WLEDs can overcome the problem of whole-organic-material WLEDs. However, the external quantum efficiency (EQE) of WLEDs based on semiconductor quantum dots is still not ideal. For example, EQE of WLED with CdSe nanocrystal as light-emitting layer is only 0.0013%.<sup>[10]</sup> Furthermore, semiconductor quantum dots usually contain toxic heavy metals, which hamper their further development.<sup>[8,11–13]</sup>

Graphene quantum dots (GQDs), one kind of carbon dots derived from graphite, are superior to semiconductor quantum dots due to their low toxicity, high chemical stability, and excellent carrier transport mobility.<sup>[14,15]</sup> Furthermore, the abundant functional groups such as carboxyl, hydroxyl, and epoxy groups on GQDs endow them with good dispersion in water and some organic solvents, and thus make them easy for the further functionalization with polymers or organic molecules in the process of constructing light-emitting diodes (LEDs) devices.<sup>[16,17]</sup> Although yellow fluorescent GQDs<sup>[17]</sup> or carbon dots<sup>[18]</sup> have been used as emitting layers to fabricate WLEDs, the luminance and current density are too low. Moreover, white light emission of previous reports results from combination of separate dopants or multiple components, which often causes phase separation and color variation.<sup>[19,20]</sup> Single-phase white-light-emitting phosphors are attracting great interests because of their high color stability and luminous efficiency for WLEDs.<sup>[21–28]</sup> Therefore, it is highly urgent to develop a novel kind of carbon-based single-phase white-light-emitting phosphor for WLEDs with enhanced performance.

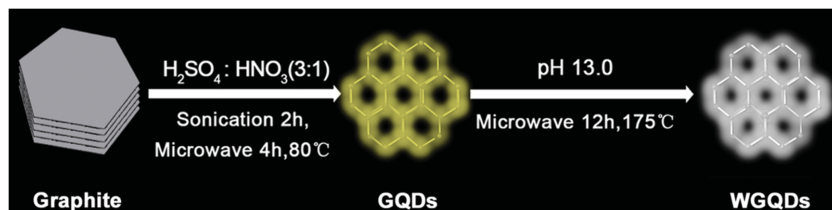
In this work, white-light-emitting graphene quantum dots (WGQDs) were prepared by a facile two-step microwave-assisted hydrothermal method (Scheme 1). Yellow-green fluorescent GQDs were synthesized beforehand through exfoliation of oxidized graphite under the ultrasonication and microwave irradiation. After that, the prepared GQDs were further treated through microwave reaction under alkaline condition (pH 13.0), giving rise to GQDs with white-light emission (WGQDs). WGQDs were subsequently used as a phosphor to fabricate WLED device by a solution-processing method. WLED based

Dr. Z. Luo, G. Qi, K. Chen, M. Zou, Dr. L. Yuwen,  
Dr. X. Zhang, Prof. W. Huang, Prof. L. Wang  
Key Laboratory for Organic Electronics and Information  
Displays & Institute of Advanced Materials (IAM)  
National Jiangsu Synergistic Innovation Center  
for Advanced Materials (SICAM)  
Nanjing University of Posts & Telecommunications  
9 Wenyuan Road, Nanjing 210023, P. R. China  
E-mail: iamwhuang@njupt.edu.cn; xwzhang@njupt.edu.cn;  
iamlhwang@njupt.edu.cn



Prof. W. Huang  
Key Laboratory of Flexible Electronics (KLOFE)  
& Institute of Advanced Materials (IAM)  
National Jiangsu Synergistic Innovation Center  
for Advanced Materials (SICAM)  
Nanjing Tech University (NanjingTech)  
30 South Puzhu Road, Nanjing 211816, P. R. China

DOI: 10.1002/adfm.201505044



**Scheme 1.** Schematic presentation of preparing WGQDs.

on WGQDs displays evidently better white electroluminescence performance than that of the previously reported WLED based on graphene quantum dots or carbon dots.

## 2. Results and Discussion

The morphology, structure, and composition of GQDs and WGQDs were characterized by transmission electron microscope (TEM), high-resolution transmission electron microscope (HRTEM), atomic force microscopy (AFM), Raman and X-ray photoelectron spectroscopy (XPS), and FTIR (Fourier transform infrared) spectroscopy. The TEM image of GQDs shows their average lateral size of 2.5 nm (Figure S1, Supporting Information), and the average height of GQDs is calculated to be about 2 nm from the AFM height image (Figure S2, Supporting Information). After further reaction under microwave irradiation in alkaline solution, GQDs were converted to WGQDs. As shown from the TEM images (Figure 1a), the lateral size of WGQDs still keeps about 2–5 nm. AFM height image of WGQDs (Figure S3, Supporting Information) evaluates that the height of WGQDs is about 1.25–2.75 nm, indicating that the as-prepared WGQDs are consisted of multilayer (two to five layer) graphene.<sup>[29,30]</sup> The crystal lattice spacing of 0.335 nm can be clearly observed in the HRTEM image of WGQDs (Figure 1b), which is assignable to the interspacing of the (002) crystal plane of graphite.<sup>[31,32]</sup>

Raman spectra of GQDs (Figure S4a, Supporting Information) and WGQDs (Figure 1c) show two peaks at 1340 and 1573  $\text{cm}^{-1}$ , which can be ascribed to the D and G bands of graphene structure respectively.<sup>[33,34]</sup> Compared to the intensity ratio of D and G bands of GQDs ( $I_D/I_G = 0.99$ ),  $I_D/I_G$  of WGQDs (0.84) is lower, indicating the decrease of defects in the WGQDs after microwave reaction under 175  $^{\circ}\text{C}$ .<sup>[33,34]</sup> Deconvolution of high-resolution C1s XPS spectrum (Figure 1d) illustrates the binding energy peaks at 284.5 (C–C), 286.0 (C–O), and 288.3 eV (O–C=O), indicating the surface oxidation of graphene in the process of preparation of WGQDs.<sup>[35,36]</sup> Binding energy peak at 284.5 and 532 eV (Figure S4b, Supporting Information, and Figure 2a), corresponding to C1s and O1s, respectively,

confirmed that the element compositions of GQDs and WGQDs are C and O.<sup>[35]</sup> FTIR spectrum of WGQDs (Figure 2b) displays the absorption bands at 1727, 1627, and 1387  $\text{cm}^{-1}$ , which can be ascribed to C=O vibration in carboxyl group, aromatic stretching vibration of graphitic domains, and O–H deformation of C–OH, respectively.<sup>[37,38]</sup> The functional groups in WGQDs are of importance for fabrication of LEDs

device through solution-based process.

The optical properties of GQDs and WGQDs were investigated by ultraviolet–visible (UV–vis) and photoluminescence (PL) spectra. GQDs prepared in the first step show the absorption peaks at 228, 262, and 306 nm, as shown in Figure S5 (Supporting Information). Two strong absorption peaks at 228 and 262 nm can be assigned to  $\pi$ – $\pi^*$  transition of  $sp^2$  domain in GQDs.<sup>[35,39]</sup> A weak shoulder peak at 306 nm can be ascribed to  $n$ – $\pi^*$  transition of oxygen-containing functional group (C=O).<sup>[39,40]</sup> After further reaction at 175  $^{\circ}\text{C}$  under microwave irradiation, UV–vis spectrum of the resultant WGQDs (Figure 3a) is absence of the absorption peak of 228 nm, which indicates that GQDs are further hydrothermally reduced under high temperature to form WGQDs.<sup>[41,42]</sup> A fluorescent emission peak of 512 nm can be observed for GQDs at the excitation of 365 nm in Figure S5 (Supporting Information). However, when the colloidal solution of WGQDs is excited at 365 nm, the PL

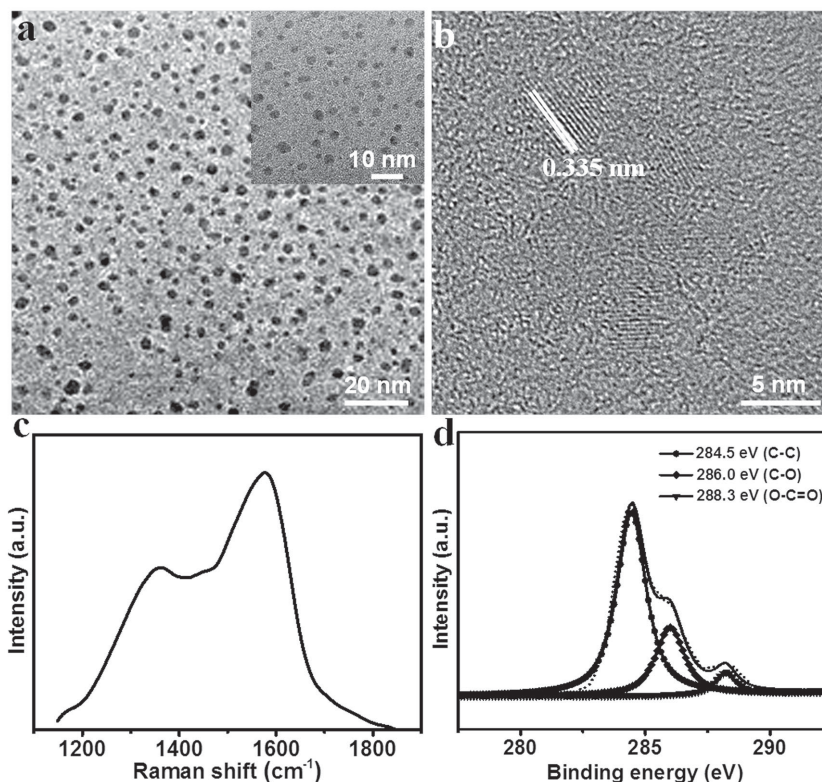


**Figure 1.** a) TEM and b) HRTEM images of WGQDs (the inset in panel (a) is the magnified TEM image of WGQDs). c) Raman characterization and d) high-resolution C1s XPS spectrum of WGQDs.

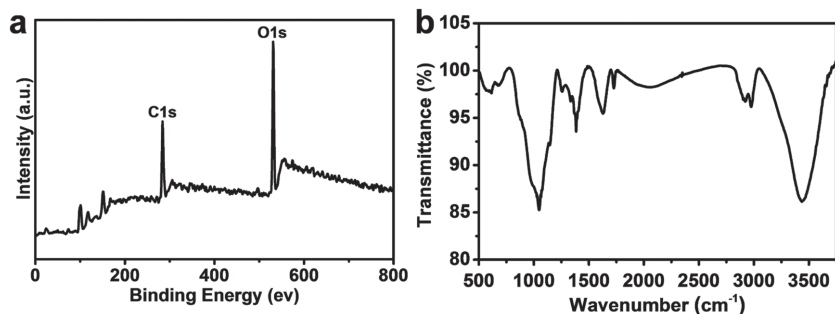


**Figure 2.** a) XPS survey spectrum and b) FTIR spectrum of WGQDs.

spectrum exhibits a broad emission band at 445 nm along with a relatively weak peak at 575 nm (Figure 3b). The white fluorescent emission of the WGQDs aqueous solution at the excitation of 365 nm can be evidently seen in the inset of Figure 3b. The excitation wavelength-dependent emission of WGQDs was also recorded through fluorescent measurement. It can be observed from Figure 3c that the fluorescent intensity of WGQDs decreases with the change of the excitation wavelength from 325 to 400 nm. The fluorescent lifetime of WGQDs was detected by the time-resolved fluorescence decay with single photon counting. Time-resolved fluorescence decay spectrum at the emission of 450 nm is shown in Figure 3d, indicating two lifetime components, i.e., 8.0 and 1.8 ns, with the amplitude of 5.6% and 94.4%, respectively.<sup>[43]</sup>

Band gap of WGQDs was measured by electrochemical method.<sup>[44–46]</sup> From Figure S6 (Supporting Information), the highest occupied molecular orbital (HOMO) and lowest unoccupied molecular orbital (LUMO) energy levels of WGQDs are calculated to be  $-5.4$  and  $-4.3$  eV, respectively. While the HOMO and LUMO energy levels of GQDs were determined to be  $-5.3$  and  $-4.0$  eV, respectively. The band gap of WGQDs (1.1 eV) is narrower than that of GQDs (1.3 eV). Solution-processed WLED was fabricated using WGQDs as single-phase white-light-emitting phosphors, and the device performance was evaluated for lighting. A schematic structure of WLED device is shown in the inset of Figure 4a. The device consists of a patterned ITO anode, a 40 nm poly (ethylenedioxythiophene):polystyrene sulfonate (PEDOT:PSS) hole injection layer, a 39 nm WGQDs doped 4,4-bis(carbazol-9-yl) biphenyl (CBP) emitting layer, a 40 nm 1,3,5-tris(N-phenylbenzimidazol-2-yl) benzene (TPBI) electron transport layer, a 0.8 nm LiF and 100 nm aluminum double layer as the cathode. The schematic energy-level diagram of the device is shown in Figure 4b. The energy transfer process from CBP to WGQDs is typically significant for bright WLED.<sup>[17]</sup> Figure 4a shows the current density–voltage ( $J$ – $V$ ) curve of the WLED. The turn-on voltage is about 5 V. The current density dramatically increases with the change of the driven voltage from 5 to 10 V, and then

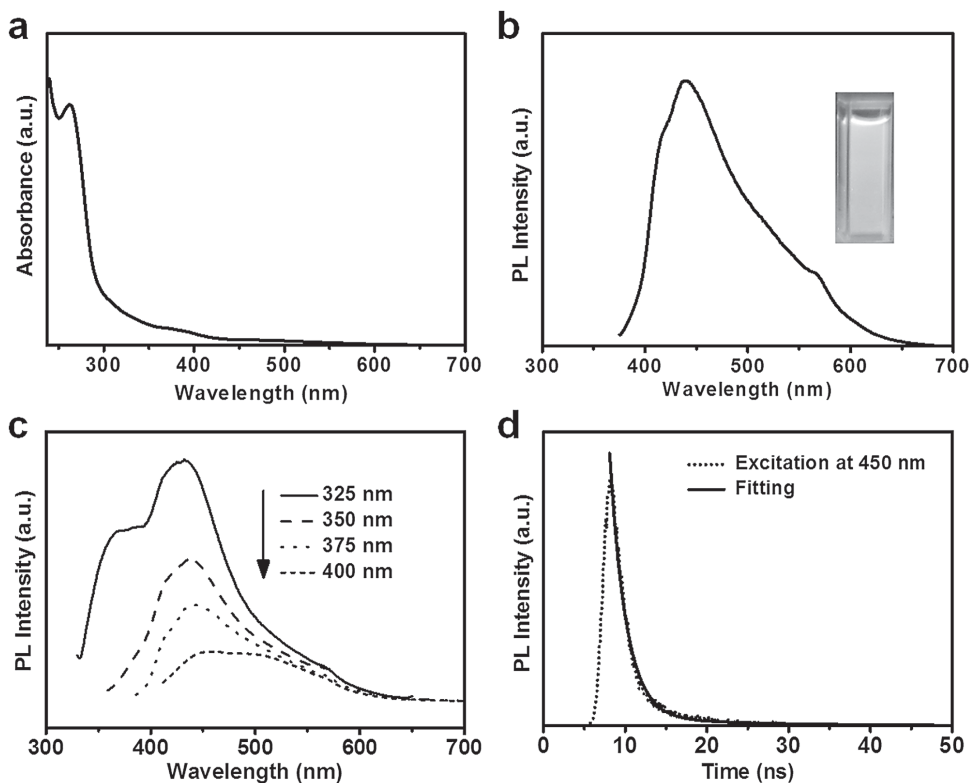


**Figure 3.** a) UV and b) PL spectra of WGQDs (the inset is the fluorescent image of WGQD aqueous solution at the excitation wavelength of 365 nm). c) PL spectra of WGQDs with different excitation wavelength. d) Fluorescent lifetime of WGQDs at the excitation wavelength of 450 nm.

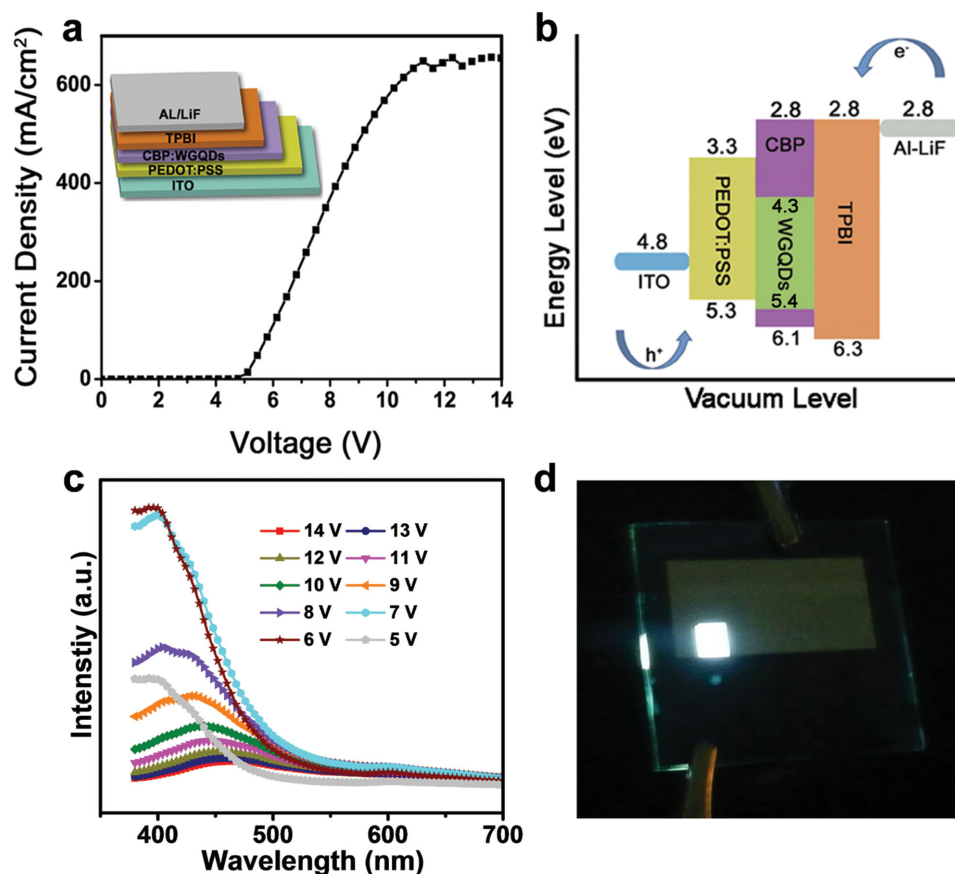


**Figure 4.** Characteristics of WLED based on WGQDs. a) Current density–voltage ( $J$ – $V$ ) and b) schematic energy-level diagram of the device (the inset in panel (a) is the schematic structure of WLED device). c) Electroluminescent spectra of the WGQDs-based WLED with applied voltages from 5 to 14 V. d) Photograph of white electroluminescence of the device operated at 14 V.

the current density is stable around  $650 \text{ mA cm}^{-2}$  in the range of 11–14 V. The evident blue light is emitted in this diode at the relatively lower voltage (5–8 V) (Figure 4c). When the voltage increases up to 11 V, the color of electroluminescence turns to white (Figure 4c). White light is emitted at 11–14 V in this device. White electroluminescence of WLED at 14 V can be clearly observed in the photograph (Figure 4d). The electroluminescent spectra of WLED (Figure 5a) display two main peaks at 450 and 600 nm, respectively. The relative intensity at 600 nm increases with the increase of applied voltage from 11 to 14 V (Figure 5a). The maximum luminance of WLED shown in Figure 5b appears to be about  $300 \text{ cd m}^{-2}$  at 8.5 V with blue light emitting. The electroluminescence of this device decays slightly from 11 to 14 V, but the luminance of white electroluminescence is still over  $200 \text{ cd m}^{-2}$ , which is higher than that of white light from LED based on yellow fluorescent GQDs.<sup>[17]</sup> The Commission Internationale de l'Enclairage (CIE) coordinates of white light from WLED in Figure 5c are (0.24, 0.25), (0.25, 0.27), (0.26, 0.28), and (0.27, 0.29) for applied voltages of 11, 12, 13, and 14 V, respectively. The CIE of WLED at the applied voltage of 14 V is near to that of pure white light (0.33, 0.33). EQEs of WLED (Figure 5d) are 0.24%, 0.21%, 0.20%, and 0.19% for 11, 12, 13, and 14 V applied voltages, respectively. To the best of our knowledge, it is the highest EQE of white light among LEDs based on GQDs,<sup>[17]</sup> ZnO-graphene quantum

dots,<sup>[47]</sup> or carbon dots,<sup>[18]</sup> although it is still lower than that of white-light-emitting LED fabricated by organic molecular phosphors.<sup>[5]</sup> The improved white electroluminescence of WLED based on WGQDs may be originated from an effective energy transfer between CBP and WGQDs because the fluorescent emission of CBP (Figure S7, Supporting Information) can be efficiently transfer to WGQDs as excitation energy.<sup>[48]</sup> It is convinced for us that enhanced white electroluminescence of WLED through WGQDs as light-emitting phosphor will shed light on more researches and applications about WLED based on nonmetal quantum dots colloidal solution because of their nontoxicity and high stability.

### 3. Conclusions

In summary, WGQDs were prepared by a facile microwave-assisted hydrothermal method. The as-prepared WGQDs display diexponential characteristic of fluorescent decay. The WLED device was constructed by solution-processing method using WGQDs as the light-emitting phosphor. The WLED based on WGQDs feature high current density and luminance at the applied voltage of 11–14 V. The CIE of white light from WLED is close to pure white light. Due to its photochemical stability and nontoxicity of WGQDs, WGQDs using as a

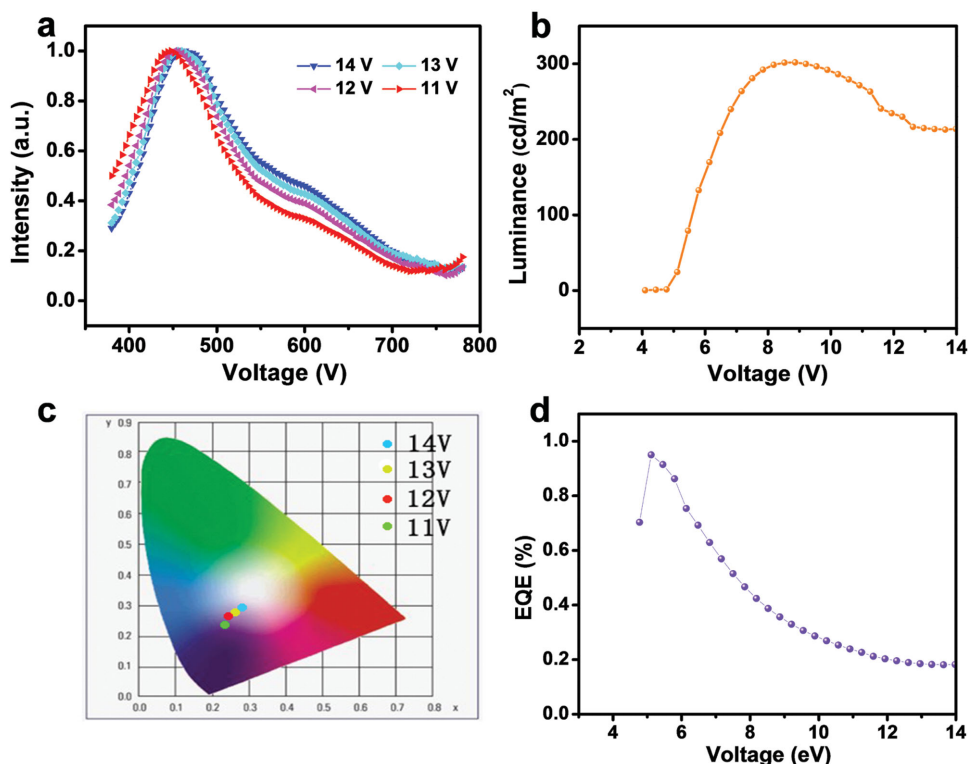


**Figure 5.** a) Electroluminescent spectra of the device with applied voltages from 11 to 14 V. b) Luminance of WLED. c) CIE1931 coordinates of white emission from the same WLED with different applied voltages from 11 to 14 V. d) EQE of WLED.

single-phase white-light-emitting phosphor are expected to be a highly efficient avenue to improve the performance of WLED based on carbon nanomaterials.

#### 4. Experimental Section

**Preparation of WGQDs:** 50 mg nanosized graphite was added into 40 mL of the mixed acid ( $\text{HNO}_3:\text{H}_2\text{SO}_4 = 1:3$ ), and then the solutions were ultrasonicated for 2 h. The dispersion was reacted for 4 h at 100 °C under the microwave irradiation. The resultant dispersion was filtered by the microporous membrane (pore size 220 nm) and neutralized with sodium carbonate. 160 mL deionized water was added for diluting the neutralized solution, and the GQDs aqueous solution was gained by dialysis with dialysis bag (molecular weight cutoff 1000). The pH value of GQDs solution was adjusted to be 13.0 and 15 mL of this GQDs solution was reacted for 8 h at 200 °C under microwave irradiation. After further dialysis (molecular weight cutoff 1000) for 3 d, the WGQDs aqueous solution was placed in refrigerator for LED device.

**Fabrication of WLEDs:** First, the patterned ITO substrate was spin-coated by a layer of PEDOT:PSS with the thickness of 40 nm according to our previously reported method in the literature.<sup>[49]</sup> The pretreatment of ITO is the same as that of literature.<sup>[49]</sup> Second, 4,4'-bis(carbazol-9-yl)biphenyl (CBP) in chlorobenzene (15 mg mL<sup>-1</sup>) and WGQDs (4 mg mL<sup>-1</sup>) in toluene with the proportion of 9:1 (w/w) were mixed together and formed the suspension. The suspension containing CBP and WGQDs was spin-coated on the layer of PEDOT:PSS, and then annealed at 80 °C for 20 min to remove solvent for forming the emissive layer with the thickness of 39 nm.<sup>[49]</sup> ITO coated with PEDOT:PSS, CBP, and WGQDs was transferred to a thermal evaporator chamber and then successively deposited with 1,3,5-tri(phenyl-2-benzimidazolyl)-benzene (TPBI) (40 nm), LiF (0.8 nm), and Al (100 nm) under pressure of  $5 \times 10^{-4}$  Pa

by thermal evaporation.<sup>[49]</sup> The luminance and  $J$ - $V$  characteristics of LED were detected using a Keithley source-meter (model 2602) combined with a calibrated luminance meter. Electroluminescence spectra were recorded by a Spectra Scan PR-670 spectroradiometer. The thickness was measured with a spectroscopic ellipsometry ( $\alpha$ -SE, J.A. Woollam Co. Inc.). All the measurements were carried out at room temperature under ambient conditions.

**Measurement of HOMO and LUMO Energy Levels of WGQDs:** In order to estimate the HOMO and LUMO energy levels of WGQDs, cyclic voltammetry (CV) measurement was conducted by establishing a standard three electrode system, composed of a glassy carbon electrode as the working electrode, a platinum wire as the counter electrode, and a saturated calomel electrode (SCE) as the reference electrode.<sup>[45]</sup> CV was recorded at a scan rate of 0.1 V s<sup>-1</sup> in the DMF containing WGQDs and 0.1 M  $(\text{Bu})_4\text{NBF}_4$  as the supporting electrolyte. The HOMO and LUMO energy levels of WGQDs were calculated from the following equations<sup>[44-46]</sup>

$$E_{(\text{HOMO})} = -e (E_{\text{ox}} + 4.74) (\text{eV}) \quad (1)$$

$$E_{(\text{LUMO})} = -e (E_{\text{red}} + 4.74) (\text{eV}) \quad (2)$$

$E_{\text{ox}}$  and  $E_{\text{red}}$  are the onset of oxidation and reduction potential, respectively. From Figure S6 (Supporting Information),  $E_{\text{ox}}$  (WGQDs) = 0.69 V (vs SCE),  $E_{\text{red}}$  (WGQDs) = -0.48 V (vs SCE),  $E_{\text{ox}}$  (GQDs) = 0.59 V (vs SCE),  $E_{\text{red}}$  (GQDs) = -0.69 V (vs SCE).

**Characterizations:** The morphology of GQDs and WGQDs was observed by TEM and HRTEM (JEOL JEM-2100F). Raman spectra were obtained by Renishaw InVia microscope with 532 nm laser beam as the excitation source. FTIR spectra were recorded with Shimadzu IRPrestige-21FTIR spectrophotometer. XPS investigation was conducted using PHI 5000 VersaProbe system with Al cathode as the X-ray source. UV-vis and

fluorescent spectra were recorded by Shimadzu UV-3600 UV-VIS NIR spectrophotometer and Shimadzu RF-5301PC spectrofluorophotometer, respectively. Fluorescent lifetime was obtained by Edinburgh FLSP920 lifetime spectrometer using picosecond laser diodes as the source of excitation.

## Supporting Information

Supporting Information is available from the Wiley Online Library or from the author.

## Acknowledgements

This work was supported by the National Basic Research Program of China (2012CB933301), the National Natural Science Foundation of China (21475064, 61204048), the Ministry of Education of China (20123223110007), the Priority Academic Program Development of Jiangsu Higher Education Institutions (PAPD), Program for Changjiang Scholars and Innovative Research Team in University (IRT\_15R37), and China Postdoctoral Science Foundation (2013M541700).

Received: November 24, 2015

Revised: December 10, 2015

Published online: February 8, 2016

- [1] H. S. Jang, H. Yang, S. W. Kim, J. Y. Han, S. G. Lee, D. Y. Jeon, *Adv. Mater.* **2008**, *20*, 2696.
- [2] S. Reineke, F. Lindner, G. Schwartz, N. Seidler, K. Walzer, B. Lüssem, K. Leo, *Nature* **2009**, *459*, 234.
- [3] P. Waltereit, O. Brandt, A. Trampert, H. Grahn, J. Menniger, M. Ramsteiner, M. Reiche, K. Ploog, *Nature* **2000**, *406*, 865.
- [4] G. M. Farinola, R. Ragni, *Chem. Soc. Rev.* **2011**, *40*, 3467.
- [5] M. C. Gather, A. Köhnen, K. Meerholz, *Adv. Mater.* **2011**, *23*, 233.
- [6] B. Zhang, G. Tan, C. S. Lam, B. Yao, C. L. Ho, L. Liu, Z. Xie, W. Y. Wong, J. Ding, L. Wang, *Adv. Mater.* **2012**, *24*, 1873.
- [7] H. S. Chen, S. J. Wang, C. J. Lo, J. Y. Chi, *Appl. Phys. Lett.* **2005**, *86*, 131905.
- [8] Q. Dai, C. E. Duty, M. Z. Hu, *Small* **2010**, *6*, 1577.
- [9] B. N. Pal, Y. Ghosh, S. Brovelli, R. Laocharoensuk, V. I. Klimov, J. A. Hollingsworth, H. Htoon, *Nano Lett.* **2011**, *12*, 331.
- [10] T. Oyamada, Y. Kawamura, T. Koyama, H. Sasabe, C. Adachi, *Adv. Mater.* **2004**, *16*, 1082.
- [11] Y. Zhang, C. Xie, H. Su, J. Liu, S. Pickering, Y. Wang, W. W. Yu, J. Wang, Y. Wang, J. Hahn, *Nano Lett.* **2010**, *11*, 329.
- [12] M. Gao, B. Richter, S. Kirstein, *Adv. Mater.* **1997**, *9*, 802.
- [13] Y. Li, A. Rizzo, R. Cingolani, G. Gigli, *Adv. Mater.* **2006**, *18*, 2545.
- [14] Y. Li, Y. Hu, Y. Zhao, G. Shi, L. Deng, Y. Hou, L. Qu, *Adv. Mater.* **2011**, *23*, 776.
- [15] J. Shen, Y. Zhu, X. Yang, C. Li, *Chem. Commun.* **2012**, *48*, 3686.
- [16] V. Gupta, N. Chaudhary, R. Srivastava, G. D. Sharma, R. Bhardwaj, S. Chand, *J. Am. Chem. Soc.* **2011**, *133*, 9960.
- [17] W. Kwon, Y.-H. Kim, C.-L. Lee, M. Lee, H. C. Choi, T.-W. Lee, S.-W. Rhee, *Nano Lett.* **2014**, *14*, 1306.
- [18] F. Wang, Y. Chen, C. Liu, D. Ma, *Chem. Commun.* **2011**, *47*, 3502.
- [19] Y. Liu, M. Pan, Q.-Y. Yang, L. Fu, K. Li, S.-C. Wei, C.-Y. Su, *Chem. Mater.* **2012**, *24*, 1954.
- [20] H. A. Höpfe, *Angew. Chem. Int. Ed.* **2009**, *48*, 3572.
- [21] G. Li, D. Geng, M. Shang, Y. Zhang, C. Peng, Z. Cheng, J. Lin, *J. Phys. Chem. C* **2011**, *115*, 21882.
- [22] M. Roushan, X. Zhang, J. Li, *Angew. Chem. Int. Ed.* **2012**, *124*, 451.
- [23] M. Shang, C. Li, J. Lin, *Chem. Soc. Rev.* **2014**, *43*, 1372.
- [24] T. Ghosh, E. Prasad, *J. Phys. Chem. C* **2015**, *119*, 2733.
- [25] R. Sekiya, Y. Uemura, H. Murakami, T. Haino, *Angew. Chem. Int. Ed.* **2014**, *53*, 5619.
- [26] X. Li, Y. Liu, X. Song, H. Wang, H. Gu, H. Zeng, *Angew. Chem. Int. Ed.* **2015**, *54*, 1759.
- [27] X. Li, M. Rui, J. Song, Z. Shen, H. Zeng, *Adv. Funct. Mater.* **2010**, *20*, 2255.
- [28] J. Song, S. A. Kulinich, J. Li, Y. Liu, H. Zeng, *Angew. Chem. Int. Ed.* **2015**, *127*, 472.
- [29] X. Zhou, X. Huang, X. Qi, S. Wu, C. Xue, F. Y. Boey, Q. Yan, P. Chen, H. Zhang, *J. Phys. Chem. C* **2009**, *113*, 10842.
- [30] A. K. Geim, K. S. Novoselov, *Nat. Mater.* **2007**, *6*, 183.
- [31] D. Deng, J. Y. Lee, *Angew. Chem. Int. Ed.* **2009**, *48*, 1660.
- [32] T. F. Yeh, J. M. Syu, C. Cheng, T. H. Chang, H. Teng, *Adv. Funct. Mater.* **2010**, *20*, 2255.
- [33] I. K. Moon, J. Lee, R. S. Ruoff, H. Lee, *Nat. Commun.* **2010**, *1*, 73.
- [34] K. N. Kudin, B. Ozbas, H. C. Schniepp, R. K. Prud'Homme, I. A. Aksay, R. Car, *Nano Lett.* **2008**, *8*, 36.
- [35] D. Pan, J. Zhang, Z. Li, M. Wu, *Adv. Mater.* **2010**, *22*, 734.
- [36] Y. Li, Y. Hu, Y. Zhao, G. Shi, L. Deng, Y. Hou, L. Qu, *Adv. Mater.* **2011**, *23*, 776.
- [37] A. Ramadoss, S. J. Kim, *Carbon* **2013**, *63*, 434.
- [38] Z. Luo, L. Yuwen, B. Bao, J. Tian, X. Zhu, L. Weng, L. Wang, *J. Mater. Chem.* **2012**, *22*, 7791.
- [39] Q. Li, S. Zhang, L. Dai, L.-s. Li, *J. Am. Chem. Soc.* **2012**, *134*, 18932.
- [40] S. K. Cushing, M. Li, F. Huang, N. Wu, *ACS Nano* **2013**, *8*, 1002.
- [41] G. Eda, Y.-Y. Lin, C. Mattevi, H. Yamaguchi, H.-A. Chen, I.-S. Chen, C.-W. Chen, M. Chhowalla, *Adv. Mater.* **2010**, *22*, 505.
- [42] L. Tang, R. Ji, X. Cao, J. Lin, H. Jiang, X. Li, K. S. Teng, C. M. Luk, S. Zeng, J. Hao, *ACS Nano* **2012**, *6*, 5102.
- [43] J. Saltiel, D. Eaker, *J. Am. Chem. Soc.* **1984**, *106*, 7624.
- [44] Y. Li, Y. Cao, J. Gao, D. Wang, G. Yu, A. J. Heeger, *Synth. Met.* **1999**, *99*, 243.
- [45] F. Wang, Y. Chen, C. Liu, D. Ma, *Chem. Commun.* **2011**, *47*, 3502.
- [46] S. Zhu, Q. Meng, L. Wang, J. Zhang, Y. Song, H. Jin, K. Zhang, H. Sun, H. Wang, B. Yang, *Angew. Chem. Int. Ed.* **2013**, *125*, 4045.
- [47] D. I. Son, B. W. Kwon, D. H. Park, W.-S. Seo, Y. Yi, B. Angadi, C.-L. Lee, W. K. Choi, *Nat. Nanotechnol.* **2012**, *7*, 465.
- [48] T. Oyamada, Y. Kawamura, T. Koyama, H. Sasabe, C. Adachi, *Adv. Mater.* **2004**, *16*, 1082.
- [49] F. Wang, J. Hu, X. Cao, T. Yang, Y. Tao, L. Mei, X. Zhang, W. Huang, *J. Mater. Chem. C* **2015**, *3*, 5533.